Received: 17 February 2020 | Revised: 24 March 2020 | Accepted: 29 March 2020

DOI: 10.1002/jsid.904

WILEY

SPECIAL SECTION PAPER

Wide-view augmented reality display with diffractive cholesteric liquid crystal lens array

Jianghao Xiong SID Student Member | **Guanjun Tan** | **Tao Zhan SID Student Member** | **Shin-Tson Wu SID Fellow**

College of Optics and Photonics, University of Central Florida, Orlando, Florida, USA

Correspondence
Shin-Tson Wu, College of Optics and Photonics, University of Central Florida, Orlando, FL 32816, USA.
Email: swu@creol.ucf.edu

Funding information
Intel Corporation

Abstract

A novel augmented reality display is proposed to achieve a field of view of 100°, while maintaining a good form factor with a glass-thin waveguide combiner. The out-coupler consists of an array of off-axis diffractive lenslets with extremely low f-number. A breadboard system is built and its performance characterized, combined with analysis and discussion of further improvement.

KEYWORDS

augmented reality, diffractive lens, waveguide display, wide field of view

1 | INTRODUCTION

The emerging augmented reality (AR) has attracted considerable attention and interests in both industry and academia because of its widespread application potential.[1–3] Nevertheless, the design of a see-through near-eye AR display with high optical performance and glass-type form factor is extremely challenging. The most straightforward method is to use a semitransparent combiner to blend the environment light with the display.[4,5] However, such a system ultimately encounters the issue of conserved étendue,[6] which states that a larger field of view (FOV) and eyebox require a bulky optics, which is unacceptable for wearing comfort. Waveguide displays[7–10] have so far been deemed as the most promising technique to achieve a glass-type form factor. It utilizes the total internal reflection (TIR) of light in the glass substrate to expand the overall étendue to get a large eyebox without sacrificing FOV. Light rays with different viewing angles are directly related to the different propagating angles in the waveguide. Current commercial products adopting waveguide, like Microsoft Hololens 1 and 2 and Magic Leap One, are able to achieve a horizontal FOV of about 40°, which is still too small as compared with the human vision. However, to further increase FOV is notoriously difficult in engineering. The challenge mainly comes from the TIR process, which sets a lower limit of propagating angle to maintain TIR and an upper limit to ensure good light uniformity.

In this paper, we report a novel display system that adopts the similar idea of expanding eyebox with TIR in traditional waveguide displays, but the out-coupler consists of an off-axis diffractive lens array that manifests high modulating power with an ultralow f-number (F#). The out-coupler can significantly release the burden of producing light rays with different angles on the TIR process and achieve an unprecedented diagonal FOV of 100°.

2 | SYSTEM DESIGN

As plotted in Figure 1A, traditional waveguide displays use a grating as the out-coupler. The grating diffracts a proportion of the light out of the waveguide, while the remaining part keeps propagating and repeats the process. Because the grating does not offer additional optical power, the angle of the out-coupled rays is determined by the TIR angle in the waveguide. If we note the lower and upper limit of the TIR angle as θ_{min} and θ_{max}, then the FOV can be calculated as

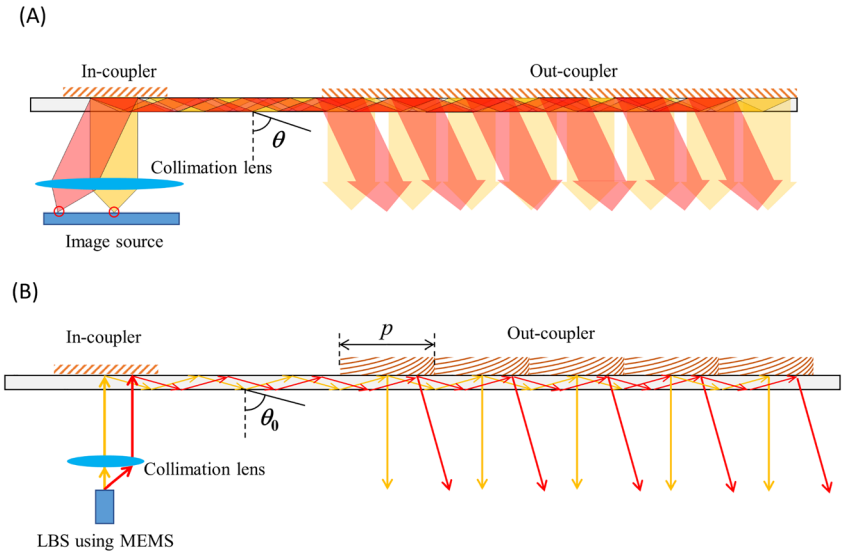

FIGURE 1 A, configuration of the traditional waveguide display. B, sketch of our proposed display system. MEMS, microelectromechanical systems

$$FOV = 2\sin^{-1}\left[\frac{1}{2}(n_s\sin\theta_{\max} - n_s\sin\theta_{\min})\right], \quad (1)$$

where n_s is the refractive index of the substrate. To estimate the theoretical FOV limit of traditional waveguide displays, it is reasonable to set $\theta_{\min}$ as the critical angle. Furthermore, we set $\theta_{\max}$ as 90° and n_s as 2.0, which are extremely challenging in practical engineering and fabrication. The FOV limit can be therefore calculated as $\text{FOV}_{\max} = 60°$. If we loosen the condition to $n_s = 1.9$ and $\theta_{\max} = 80°$, then the maximum FOV is 53°. It should be noted that the calculation is for 1D FOV. But still, the theoretical limit is far from the FOV of human vision system, which is about 90° for binocular vision.

To overcome the limit, we propose to use an off-axis diffractive lens array as the out-coupler. The configuration of our proposed display system is plotted in Figure 1B. The image source is a laser beam scanning system with a collimation lens. The propagating angle in the waveguide is thus fixed, but the relative position of each ray in the waveguide is different. So each ray will run into different portions of the lens and gets diffracted into different angles. For a single lenslet, the FOV of the system is only determined by the F# of the lens:

$$\text{FOV} = \tan^{-1}\frac{1}{2F\#}. \quad (2)$$

In theory, the FOV is not limited as long as a low F# can be achieved. For estimation, to achieve FOV beyond 60°, from Equation 2, we need F# = 0.87. Similarly, if we can reduce F# to 0.60, then FOV can be expanded to 80°.

The fabrication of our proposed lens array adopts the polarization holography system depicted in Figure 2. The system is used to produce linear polarization pattern with the interference of two opposite circularly polarized light beams. As Figure 2A depicts, the laser beam (λ = 457 nm), after filtering and expansion, is separated by the beam splitter to two paths. A quarter-wave plate is placed in each arm to convert the incident light to right-handed circular polarization (RCP) (Path 1) and left-handed circular polarization (LCP) (Path 2). An aspheric lens (L1) with focal length f_1 = 7.5 mm and diameter of 10 mm is placed in Path 1. L1 functions as the template lens to produce the desired wavefront of the diffractive lens. Another lens L2 with a long focus (f_2 = 20 cm) is placed in Path 2 to focus the light to ensure the same light intensities of two paths. Because the focal distance of L2 is much longer than that of L1, its influence on the final wavefront is negligible. A black matrix with a square whole (2 × 2 mm) is placed right before the sample to form the square-shaped lens, as shown in Figure 2B. The total output power of the laser is 100 mW, and the measured light intensity on the sample is 115 mW/cm^2.

The holography serves as the exposure system for the fabrication whose fundamental mechanism is photo-alignment of liquid crystals (LCs). With the exposure under linearly polarized light, the azobenzene photo-alignment molecules we used (brilliant yellow) tend to align perpendicular to the electric field.[11] So with adequate exposure dosage, the photoalignment layer can record the electric field pattern. When the LC is placed on top of the photoalignment layer, the LC in contact will also follow the pattern. If the employed LC is nematic, then the whole layer will follow the bottom LC molecules, as in transmission Pancharatnam–Berry optical elements.[12] However, in our fabrication, we used

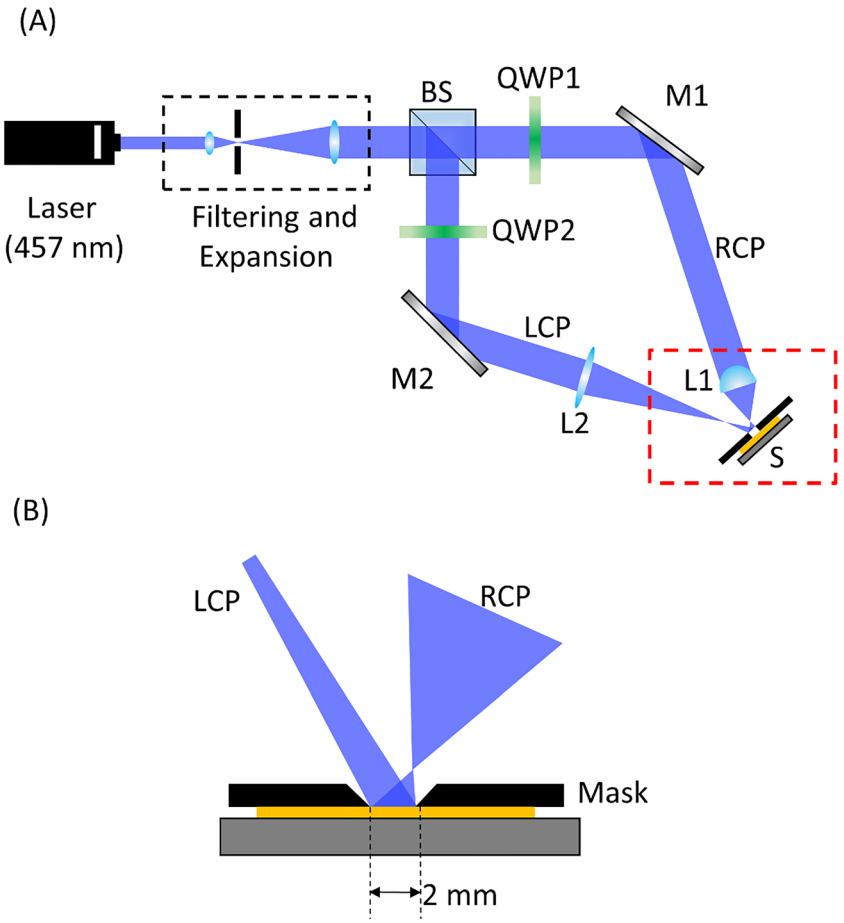

FIGURE 2 A, setup of the polarization holography system. B, enlarged part of the red dashed box in A. LCP, left-handed circular polarization; RCP, right-handed circular polarization

cholesteric LC (CLC), which tends to form helical structure. The bottom LC that follows the photoalignment pattern will give the bulk CLC a tilt angle,[13,14] as Figure 3 shows.

Our fabrication process starts with cleaning the glass substrate (1 mm thick) with ethanol, acetone, and isopropyl alcohol. After drying with air, a layer of brilliant yellow (1:500 in dimethylformamide) is spin-coated on the substrate at 500 rpm for 5 s and 3000 rpm for 30 s. Then, the sample is placed under the holography system for exposure. For each lenslet, the exposure time is 15 s, followed by translating the sample to the position of next lenslet and repeating the exposure process. The laser beam is totally blocked during the translation process to avoid damaging the pattern. After the exposure, a layer of CLC mixture is spin-coated onto the photoalignment layer. The precursor of the CLC mixture consists of 2% chiral dopant R5011, 3% photoinitiator Irg651, and 95% reactive mesogen RM257. The precursor is dissolved in the toluene at 1:7 weight ratio. The spin-coating speed is 2000 rpm for 30 s. After that, the sample is placed under the UV lamp (365 nm, 10 mW/cm^2) for 5 min to polymerize and stabilize the structure. The detailed procedure is sketched in Figure 4.

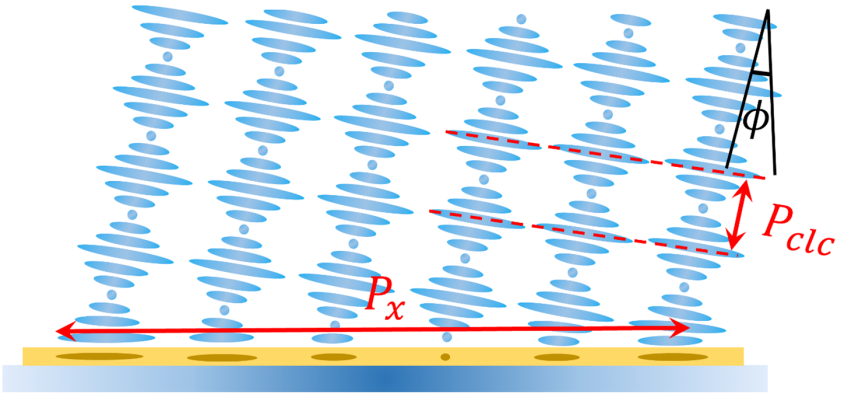

FIGURE 3 Schematic of the cholesteric liquid crystal orientation with patterned photoalignment layer

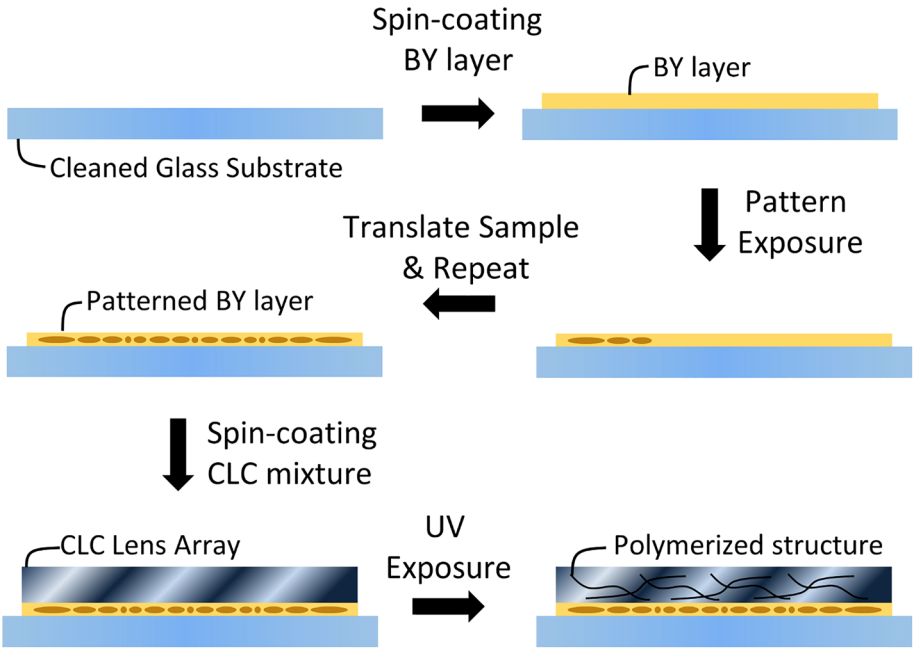

FIGURE 4 Detailed flowchart of the fabrication process. CLC, cholesteric liquid crystal

3 | RESULTS AND DISCUSSION

3.1 | CLC lens array

In experiment, we fabricated a CLC lens array with 8 × 15 lenslets. Each lenslet has a dimension of 2 × 2 mm, so the total eyebox size is about 16 × 30 mm, which is adequately large for a comfortable viewing experience. Figure 5 shows the photo of the lens array. The light from the background can pass the lens array and form a clear see-through view, which satisfies the requirement for AR displays. On the other hand, because of the off-axis feature, each lenslet forms an image of the ceiling light above.

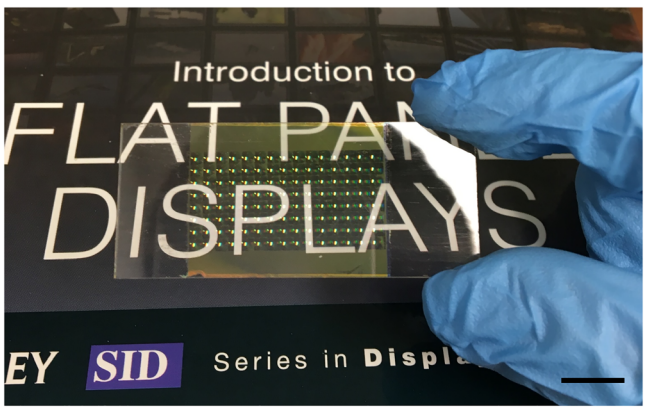

FIGURE 5 Photo of the cholesteric liquid crystal lens array. The bright spot in each lenslet is the image of the ceiling light. Scale bar: 1 cm

3.2 | Display system

The display system setup is shown in Figure 6A. The image source is a pico projector (Sony MP-CL1) using laser beam scanning. The wavelength of the red channel is 639 nm. Recall that the exposure system uses the blue light with $\lambda = 457$ nm. The effective F# is therefore calculated as 0.54. A lens is placed right after the projector to collimate the laser beam. A prism is attached onto the waveguide with index-matching oil to act as the in-coupler. The incident angle of the laser beam is adjusted to 45° to ensure that each laser beam hits the exact same location of the lenslet after each TIR. The TIR occurs in the x direction in Figure 6B, which can duplicate the image in that direction. But in the x direction, no such process can dupliate the image. In principle, the image should be duplicated in the x direction before reaching the lens array, which can be achieved by using a fold grating that simultaneously duplicates and bends the light rays. However, considering the fabrication difficulty of fold grating, we use the simple digital duplication, which means the input of a line of identical images. The trade-off is sacrificed resolution.

The image of a letter "A" is taken and shown in Figure 7. The horizontal FOV is measured as 80°. The theoretical calculation using an effective F# = 0.54 and Equation 2 gives FOV = 86°, which is close to our measured result. The horizontal FOV exceeds the 60° theoretical limit in traditional waveguide displays. Because the lens is square-shaped, the vertical FOV is the same as the horizontal one, which produces a diagonal FOV of 100°,

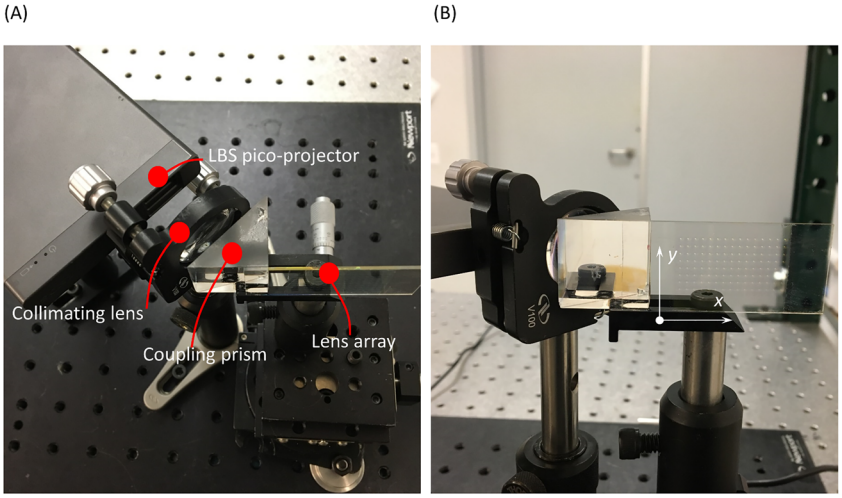

FIGURE 6 Pictures of the display system. A, top view of the display experimental setup. B, front view of the setup, showing the two directions of image duplication

which is at the same level as the current virtual reality (VR) headsets.

The image resolution is relatively low due to several reasons. The first comes from the digital replication of the image. The pico projector in the system has a resolution of 1920 by 720. But we have to replicate eight of the same images in the vertical direction. So each image has a full resolution about 90 by 90. The second reason is due to the collimation of laser beams. Although the lens can collimate the scanned laser rays in different time sequences into one direction, for each single ray, the divergence angle is actually increased. The divergence angle of the laser ray is designed to be 4.5 mrad, which promises a good depth of focus (DOF) of the projector. But after the collimation lens, the DOF of the laser beams is reduced to about 1 cm. So the laser beams hitting different portions of the lens array have different beam widths, which significantly blurs the final image. This issue can be solved by adjusting the Gaussian beam divergence angle of the laser source before it hits the microelectromechanical systems (MEMS), which, unfortunately, is rather difficult for us because the integrated photonics module is too delicate to adjust without damaging it.

The third problem, which can be observed in Figure 7, is the overlapped circle-shaped boundaries. This is actually due to the laser rays hitting the boundary of the camera pupil being diffracted. In theory, the despeckling method can be applied to reduce the coherence of the laser beams to alleviate this issue.

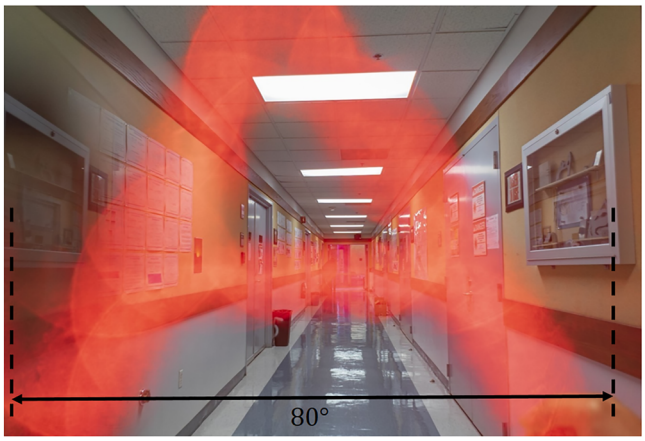

FIGURE 7 Photo of the see-through view with the display system presenting a letter "A." The horizontal field of view is measured as 80°

3.3 | Depth generation

In previous display systems, the out-coupled light rays for each pixel are parallel, which indicates that the image is located at infinity. In order to imitate the real object to obtain a more natural and comfortable viewing experience, finite depth should be supported. This can be achieved by changing the input angle, as shown in Figure 8. The red rays with propagating angle θ_0 indicate the case with infinite depth, with the rays hitting the same position of the lenslet after each TIR. If the input angle of the rays is changed so that the propagating angle becomes θ_1 (blue rays), then the rays will hit different positions of the lenslets, resulting in the diverged output rays. The depth of image plane can be calculated as

$$F = \frac{P}{\Delta\theta}\cos^2\theta_0, \tag{3}$$

where P is the pitch of the lenslet and $\Delta\theta = \theta_1 - \theta_0$.

The system implementation involves another degree of freedom (DOF) besides two DOFs for displaying 2D images. This can be achieved with various approaches. As shown in Figure 9A, for the laser scanning method,

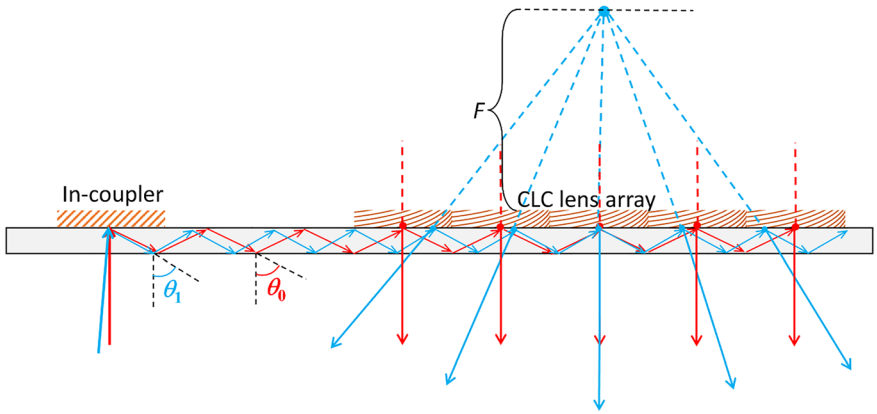

FIGURE 8 Schematics of the finite depth generation method. CLC, cholesteric liquid crystal

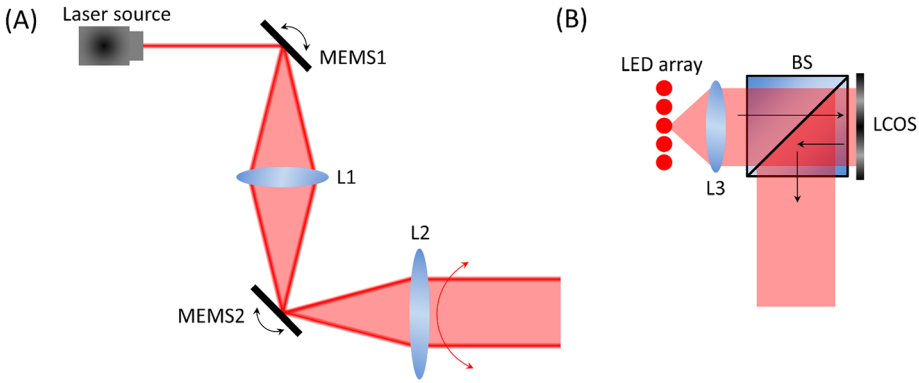

FIGURE 9 Approaches to generate collimated 2D pattern with adjustable angle. A, laser beam scanning type. B, LED array combined with LCOS. LCOS, liquid crystal on silicon; MEMS, microelectromechanical systems

after the laser source passing the 2D scanning mirror (MEMS1), a lens L1 is used to refocus the laser rays onto another 1D scanning mirror (MEMS2). Then, the laser rays are collimated by another lens L2. This way, the laser rays are distributed into a 2D parallel pattern with adjustable direction. Another approach using LED and liquid crystal on silicon (LCOS) is plotted in Figure 9B. Each LED in the array can produce different angles after collimation lens L3. Each light intensity is modulated by the LCOS. Because the light from LED is incoherent, the speckling issue can be well suppressed. However, to avoid the chromatic aberration issue, a narrow spectral bandwidth is preferred.

4 | CONCLUSION

We propose a new display system involving waveguide architecture and reflective lens array that has no theoretical limit on FOV. To prove the concept, a lens array was fabricated with CLC and polarization holography system. The display system was built and analyzed. We also discussed further improvement of the system in terms of imaging performance and 3D scene generation. This work would provide useful guidelines for designing wide FOV AR displays.

ACKNOWLEDGMENT

The authors are indebted to Intel Corporation for the financial support.

ORCID

Jianghao Xiong https://orcid.org/0000-0002-8122-9936
Shin-Tson Wu https://orcid.org/0000-0002-0943-0440

REFERENCES

1. Cakmakci O, Rolland J. Head-worn displays: A review. J Disp Technol. 2006;2(3):199–216.
2. Van Krevelen DWF, Poelman R. A survey of augmented reality technologies, applications and limitations. Int J Virtual Real. 2010;9(2):1–20.
3. Lee YH, Zhan T, Wu ST. Prospects and challenges in augmented reality displays. Virt Reality Intell Hardware. 2019;1(1):10–201.
4. Li G, Lee D, Jeong Y, Cho J, Lee B. Holographic display for see-through augmented reality using mirror-lens holographic optical element. Opt Lett. 2016;41(11):2486–2489.
5. Cheng D, Wang Y, Hua H, Sasian J. Design of a wide-angle, lightweight head-mounted display using free-form optics tiling. Opt Lett. 2011;36(11):2098–2100.
6. Singer W, Totzeck M, Gross H. Handbook of Optical Systems Wiley-VCH: Weinheim; 2005.
7. Kress BC. Optical waveguide combiners for AR headsets: Features and limitations. Proc SPIE. 2019;11062;110620J.

8. Liu Z, Pang Y, Pan C, Huang Z. Design of a uniform-illumination binocular waveguide display with diffraction gratings and freeform optics. Opt Express. 2017 2017;25(24): 30720–30731.
9. Waldern JD, Grant AJ, Popovich MM. DigiLens switchable Bragg grating waveguide optics for augmented reality applications. Proc SPIE. 2018;10676;106760G.
10. Weng Y, Zhang Y, Cui J, et al. Liquid-crystal-based polarization volume grating applied for full-color waveguide displays. Opt Lett. 2018;43(23):5773–5776.
11. Chigrinov VG, Kozenkov VM, Kwok H-S. Photoalignment of Liquid Crystalline Materials: Physics and Applications Wiley-VCH: Weinheim; 2008.
12. Lee YH, Tan G, Zhan T, et al. Recent progress in Pancharatnam–Berry phase optical elements and the applications for virtual/augmented realities. Opt Data Process Storage. 2017;3(1):79–88.
13. Xiong J, Chen R, Wu ST. Device simulation of liquid crystal polarization gratings. Opt Express. 2019;27(13):18102–18112.
14. Lee YH, He Z, Wu ST. Optical properties of reflective liquid crystal polarization volume gratings. J Opt Soc am B. 2019;36 (5):D9–D12.

AUTHOR BIOGRAPHIES

Jianghao Xiong received his BS degree in Physics from the University of Science and Technology of China (USTC) in 2017 and is currently working toward a PhD degree from the College of Optics and Photonics University of Central Florida, Orlando. His current research interests include near-eye displays and novel liquid crystal display devices.

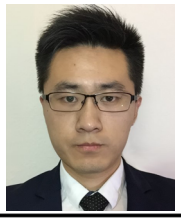

Guanjun Tan received a BS degree in Physics from the University of Science and Technology of China in 2014 and is currently working toward a PhD degree at the College of Optics and Photonics, University of Central Florida. His current research interests include head-mounted display, organic LED display, and novel liquid crystal display technologies.

Tao Zhan received his BS degree in Physics from Nanjing University in 2016 and is currently working toward a PhD degree from the College of Optics and Photonics, University of Central Florida. His current research interests include display system design, liquid crystal optical elements, and computational diffractive optics.

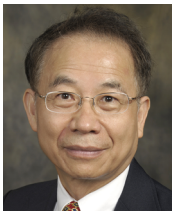

Shin-Tson Wu is a Pegasus professor at the College of Optics and Photonics, University of Central Florida. He is among the first six inductees of the Florida Inventors Hall of Fame (2014) and a Charter Fellow of the National Academy of Inventors (2012). He is a Fellow of the IEEE, OSA, SID, and SPIE and an honorary professor of Nanjing University (2013) and of National Chiao Tung University (2017). He is the recipient of 2014 OSA Esther Hoffman Beller Medal, 2011 SID Slottow-Owaki Prize, 2010 OSA Joseph Fraunhofer Award, 2008 SPIE G. G. Stokes Award, and 2008 SID Jan Rajchman Prize. Presently, he is serving as SID honors and awards committee chair.

How to cite this article: Xiong J, Tan G, Zhan T, Wu S-T. Wide-view augmented reality display with diffractive cholesteric liquid crystal lens array. *J Soc Inf Display*. 2020;28:450–456. https://doi.org/10.1002/jsid.904